Concept for Thermal Analysis of Batteries using Reduced Order Modeling

Anna Szardenings[1,2,a)], Niels Petersen[3] and Heike Fassbender[4,b)]

[1]*Volkswagen Group Components, Gifhorner Strasse 180, Brunswick, Germany*
[2]*Institute for Numerical Analysis, Technical University of Brunswick, Germany*
[3]*Technical University of Brunswick, Germany*
[4]*Institute for Numerical Analysis, Technical University of Brunswick, Germany*

[a)]Corresponding author: anna.szardenings@volkswagen.de
[b)]h.fassbender@tu-bs.de

Abstract. *Thermal management for battery systems is crucial for its performance and reliability, especially in the application of electrical vehicles. Using digital models in order to control and monitor battery systems has gained significant interest. In this work a concept for a real-time applicable model of a battery system is proposed. The model is built using various model reduction approaches. First, a high dimensional model (HDM) of a battery is set up and validated with test data. In the proposed approach the HDM is separated into a thermo-electric, a solid and a fluid model, which are coupled though input and output parameters. Different model reduction techniques and approximations are discussed for the linear solid part and non-linear fluid part. The thermal model is coupled with a thermal-electric model for the heat generation inside the battery cells.*

INTRODUCTION

The thermal behavior of battery systems limits the range and reliability of electric vehicles and is crucial for its performance. Thus, various approaches for thermal management and control have been studied for the application in electric vehicles [1, 2, 3]. One possibility to monitor and control the thermal behavior of a battery is to implement temperature sensors. This however results in a high amount of sensing units needed to map the whole battery system thermally. Further, only temperatures on the surface of the battery cells and modules can be measured, while the critical temperatures and hot spots of the system might be located inside of the cells [4, 5]. To overcome these problems some approaches have been developed to build real-time models of the battery system, including one-dimensional models with lumped masses [6]. Other battery models have been used for estimation of the battery state in terms of state of health (SOH), state of charge (SOC) or Voltage [7, 8, 9]. However these models do not include a complete overview of the thermal behavior of all components in the system.
The aim of this paper is to build a digital twin of the complete battery system, including other high voltage components such as the battery junction box and the bus bars connecting the cells as well as the cooling plate. This is done by applying model order reduction methods on a high dimensional model (HDM) of the battery system. Therefore, the digital twin is directly derived from a detailed three-dimensional model. The numerical reduction methods aim to reduce the computation time for solving the differential algebraic equation of the system. The proposed concept combines different model order reduction techniques and an electro-thermal battery model in order to effectively apply them to the large scale dynamical and multi-physical system. The real-time applicable model calculates desired temperatures at all locations of the battery system and is implemented on the battery management system (BMS). Based on those calculations the operating strategy and battery cooling can be regulated onboard [10].
There are various model order reduction techniques for linear as well as nonlinear systems that have already been effectively applied to thermal [11, 12, 13] and fluid models [14, 15, 16]. Likewise reduced order models have been used to depict the thermal behavior for single cell and battery stacks [17, 18, 19] or to calculate the electric behavior [20]. Yet, those models do not include the complete battery system with its linear and nonlinear system equations as needed in the application for a digital twin.

International Conference of Numerical Analysis and Applied Mathematics ICNAAM 2020
AIP Conf. Proc. 2425, 020007-1–020007-9; https://doi.org/10.1063/5.0081513
Published by AIP Publishing. 978-0-7354-4182-8/$30.00

However, when applying dynamic and nonlinear model order reduction techniques to larger systems, one faces several challenges.
In the presented concept the battery system is split into three parts, a thermal model, as fluid model and an electro-thermal model In that way linear model order reduction methods can be applied to the large scale thermal model of the battery system and the nonlinear fluid part is approximated through a sub model.

DESCRIPTION OF THE HIGH DIMENSIONAL BATTERY MODEL

The examined battery system consists of twelve modules consisting of a 24 cell battery stack. The modules are located in an aluminum housing and are connected in series using copper connectors. The cooling plate is located on the bottom of the housing. As cooling fluid a water-glycol mixture (50:50) is used. In addition, the battery system contains a battery junction box (BJB), a cell management controller(CMC) and a battery management system (BMS). A schematic picture of the system is shown in Figure 1.
First, a HDM of the battery system is developed and validated with test data. In the model the heat losses inside the

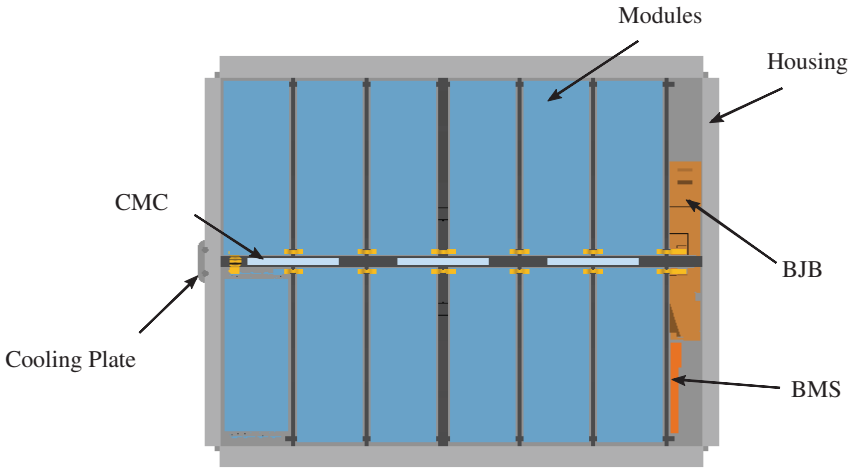

FIGURE 1. Battery system with its main components: cooling plate, housing, battery modules, battery junction box, cell management controller and battery management controller

cells are calculated using an equivalent circuit model (ECM) and ohmic heat loss in all other high voltage components. The thermal, fluid and electrical equations are solved simultaneously.

Simulation Model of the Battery Module

In this paper the validation with test data is conducted for one module and the corresponding part from the cooling plate on the bottom. Since the 12 modules in the system are alike, a smaller model can be used for a more detailed validation. The model of the battery module is shown in Figure 2. The module consists of 24 lithium-ion pouch cells. Three parallel cells are connected with copper bus bars to eight packs in serial. The cells are modeled as blocks with a direction dependent heat conduction and a copper and aluminum tab on the minus and plus side respectively. The cell stack is enclosed in an aluminum housing. The module is placed on an extracted part from the cooling plate with a thermal gap filler in between.
The HDM is developed in ANSYS Fluent ® using the multi-scale multi-dimensional (MSMD) battery model. The mesh is built using a polyhedral mesh with 12.2 million cells. The heat loss $\dot{Q}$ inside the bus bars and tabs is calculated through the temperature dependent electrical resistance $R_{\mathrm{el}}(T)$, the current draw I and the cross-section area A and length l of the connectors using Equation 1.

$$\dot{Q} = I^2 \cdot \frac{A \cdot R_{\mathrm{el}}(T)}{l} \tag{1}$$

The heat loss in the cells is calculated using an equivalent circuit model (ECM), in which the generated heat depends on the temperature, state of charge (SOC) and current draw in the cell. The ECM is described in the following section.

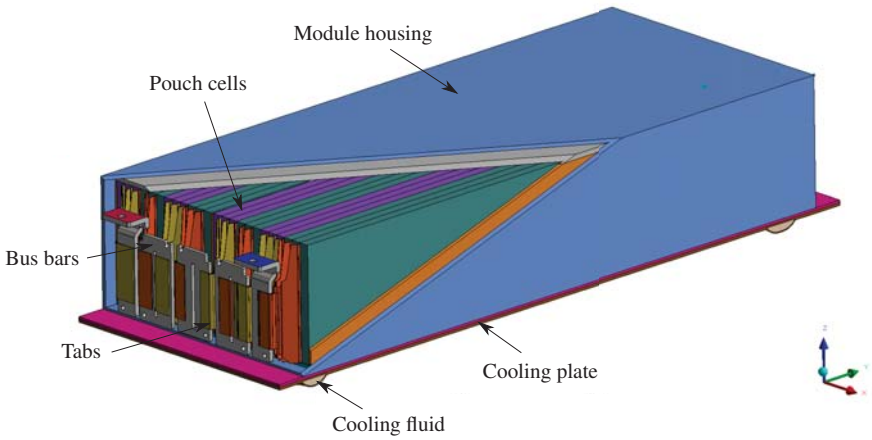

FIGURE 2. Model of the battery module with the corresponding cooling plate

Contrary to other software packages in ANSYS Fluent ® the ECM is solved at each discretized finite volume inside the battery cells. A local SOC and temperature distribution in the cells is calculated, thus, each cell volume has a certain heat source. Further the local change in the resistance inside the cell is considered and a local current distribution can be obtained. This approach has shown to approximate charge and discharge behavior in batteries with a good accuracy [21, 22]. The electrical connection between the cells, in our case three serial and eight parallel, is recognized automatically by the software.

Equivalent Circuit Model

Various approaches of multi-scale and multi-dimensional (MSMD) modeling have been developed to predict the electric, thermal and chemical behavior of lithium-ion cells. The approaches differ in their complexity, accuracy and computation time. Mainly the models can be dived into three groups, physical models, empirical models and equivalent circuit models [23].

The equivalent circuit model can be coupled with a thermal model and is therefore widely used for estimation of thermal and electrical behaviors of battery stacks. The advantages of this 0D-model are calculation speed and reliable approximation of the thermal and electrical behavior. For the model an electric circuit with temperature and SOC dependent data is built. The data is obtained by impedance spectroscopy measurements [24]. In the model the batteries electrical resistance is calculated with one ohmic resistance (R_0) and two parallel resistors (R_1 and R_2) and capacitors (C_1 and C_2) in a row as shown in Figure 3. From the voltage drop in the circuit the heat loss $\dot{Q}_{\text{cell}}$ in the cell is

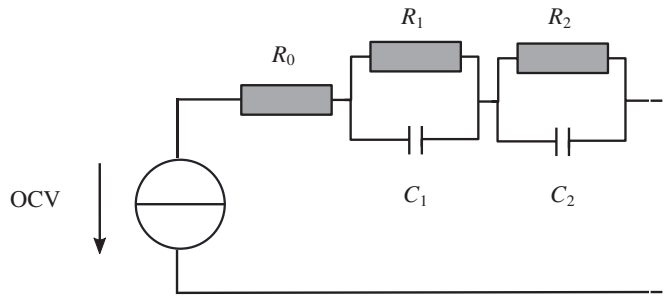

FIGURE 3. ECM with the electric resistance R_0 and the two parallel capacity and resistor pairs R_1 and C_1 and R_2 and C_2

calculated with Equation 2, where I is the current draw, V_{OC} is the open circuit voltage (OCV), V the cell voltage, T_{cell} the cell temperature and $\frac{dV_{\text{OC}}}{dT}$ the OCV change with temperature. The first term represents electric joule heating

through the cell resistance and the last term the reversible heat generated through the enthropic reactions during charging and discharging. For simplification and due to the small contribution to the overall heat the last term is neglected [23, 25, 26].

$$\begin{aligned}\dot{Q}_{\text{cell}} &= I(V_{\text{OC}} - V) - IT_{\text{cell}}\frac{dV_{\text{OC}}}{dT} \\ &\approx I(V_{\text{OC}} - V)\end{aligned} \tag{2}$$

Validation and Results

For the validation thermal measurements of one module and the cooling plate part were performed. The battery module is set up with several temperature sensors between the cells and at the bus bars as shown in Figure 4. The two sensors discussed here are marked through circles.

In the simulation model temperatures are examined at the location of the sensors. Transient simulations are carried

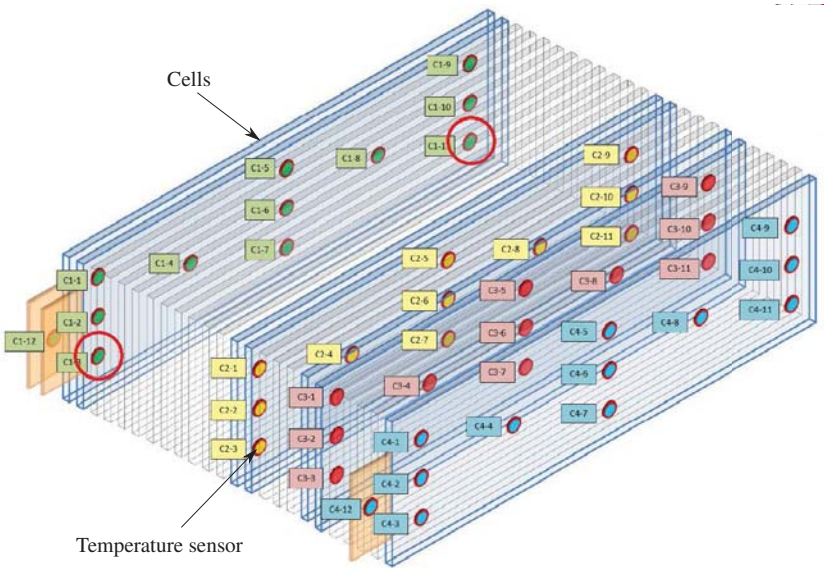

FIGURE 4. Temperatures sensor locations of the tested battery module, the sensor location C1-3 (bottom left) and C1-11 (bottom right) that are discussed for the validation are marked

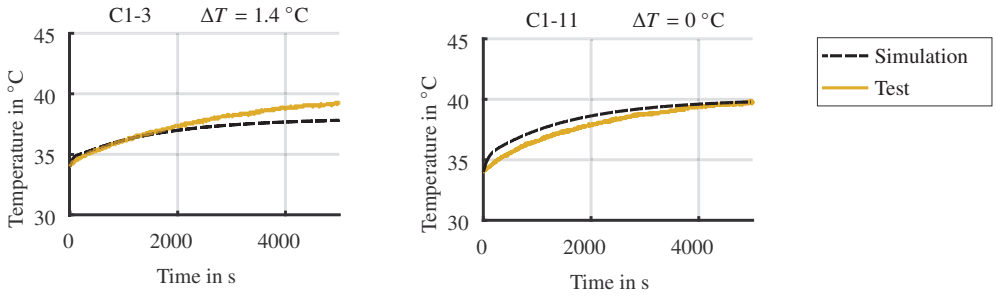

FIGURE 5. Temperatures from simulation and thermal tests over time at sensor locations on plane C1 between cell number 1 and 2 at the bottom left and right hand side

out by applying current profiles used in the tests to the model. Boundary conditions as well as fluid temperature and mass flow are defined according to the set up in the measurement. Temperature at the sensor locations are compared over time.

In Figure 5 two temperatures between the cells 1 and 2 are displayed as an example with an applied current profile of

± 240 A pulses. In this example the right side matches the measurement data at the end of the current profile, wherein on the left side some deviation can be seen.
Overall, at the end of the current profile the cell temperatures of the simulation model are 1.7 °C lower on average with a mean temperature of 38.1 °C. The bus bars reach 44.6 °C on average, being 1.6 °C lower than the temperatures from the measurements. The mean deviation between the temperatures of the simulation model compared to the measurements is 3.8 %.
The maximal temperature deviation by the end of the time slot is located on the left side on Plane C4 with $\Delta T = 5$ °C. This arises from differences in the cooling plate and flow properties compared to the measurements and can also be related to a slightly underestimated heat loss in the bus bars and tabs. On the right hand side of the plane temperatures calculated in the simulation match the measurement data. Probably here the cooling flow in the measurement could be reproduced in the simulation. Due to the accuracy of temperature sensors used in the measurement of 0.5 °C further deviations are expected. In total the model can be used to replicate the thermal behavior of a module accurately enough for the purpose.
Test data from the full battery system with 12 modules will be used to validate the detailed HDM.

REDUCED ORDER MODEL CONCEPT

In this section the concept developed for the approximation of the battery system through different techniques is described and discussed.
For the development of the reduced order model (ROM) the HDM is separated into three sub-models based on their system. A fluid model of the cooling plate, where energy and flow equations are solved, a purely thermal and linear model of the battery and an electro-thermal model as shown in Figure 6. The concept is described in the patent [27] that will be published in 2022 and which is the basis for this section.
In the electro-thermal model heat losses inside the cells, high voltage connectors and other electrical components such as the E-Box are calculated. The cooling plate model consists of the cooling plate with the channels and the cooling fluid itself. The model calculates heat transfer from the thermal system into the fluid. The thermal model includes the whole battery system without the cooling plate. Consequently, it consists only of solid parts and linear system equations. The temperatures of the system components are calculated in this model. ROM methods can be applied to the linear thermal and nonlinear fluid model separately, resulting in several advantages that will be described in the following sections.

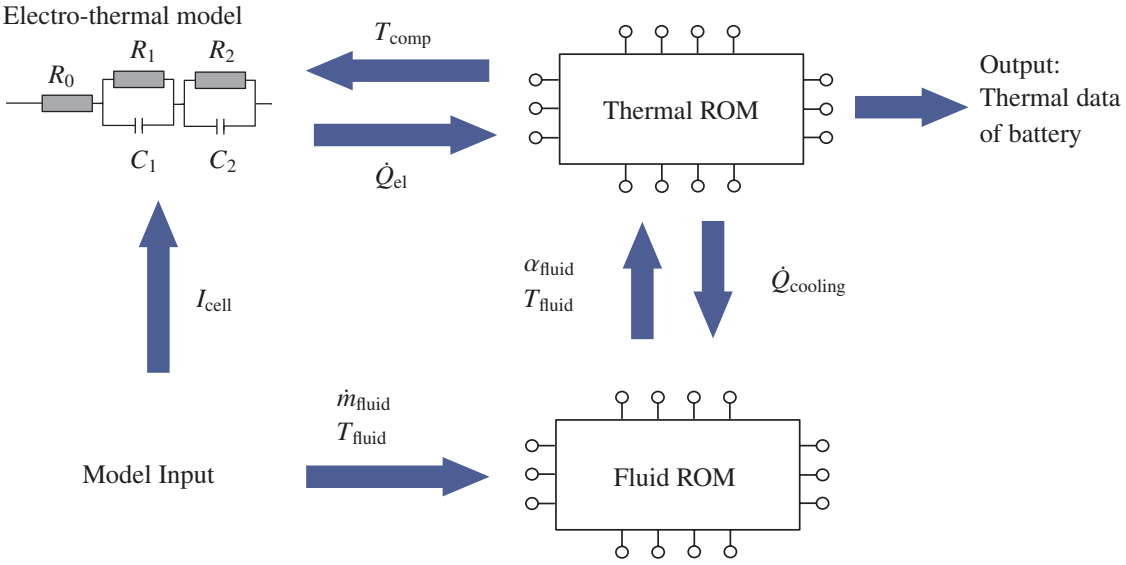

FIGURE 6. Coupling of the three sub models for the battery ROM: the electro-thermal model, the thermal ROM and the fluid ROM

Electro-thermal 0D-Model

In the electro-thermal model, heat losses from the high voltage components based on the current draw I_{cell} are computed. The calculations include the following parts:

- Solving the ECM described in the Section "Equivalent Circuit Model" and calculating the heat losses in the battery cells using the current SOC and temperature (T_{comp})
- Calculating the current distribution between the parallel cell based on the electrical resistance calculated in the ECM
- Calculating the SOC change for each cell
- Solving Equation 1 to calculate the heat losses in all other components of the current path based on their electrical resistance and temperature (T_{comp})

The resulting heat losses $\dot{Q}_{\text{el}}$ are coupled with its components in the thermal model.

Thermal Model and linear Model Reduction

The solid part of the battery system model is solved using only energy equations, since the electrical part is calculated in the 0D-model and the cooling plate is calculated separately. Therefore, the model contains only linear equations and can be modeled as a linear, time-invariant model (LTI). Thus, the main advantages in separating the thermal and fluid part is that a linear model order reduction technique can be applied. In order to reduce large scale systems linear model order reduction techniques based on singular value decomposition or Krylov subspaces have been established [28, 29, 30].
The thermal battery system model can be described by a state space model, where $x(t)$ is the state variable of length n, $u(t)$ the input vector of length m, and $y(t)$ the output vector of length p. The matrices are namely $E^{n\times n}$, the capacity matrix, $A^{n\times n}$, the system matrix, $B^{n\times m}$, the input matrix and $C^{p\times n}$ and $D^{p\times m}$ the output matrix. The size of matrices represents the dimension of the system and number of elements in a finite element model (FEM) [31].

$$\begin{aligned}\dot{\mathbf{E}}\mathbf{x}(t) =& \mathbf{A}\mathbf{x}(t) + \mathbf{B}\mathbf{u}(t)\\ \mathbf{y}(t) =& \mathbf{C}^T\mathbf{x}(t) + \mathbf{D}\mathbf{u}(t)\end{aligned} \tag{3}$$

The matrices of the system are obtained from ANSYS Mechanical ® by following the procedures explained in [28]. Simulations are conducted in steady state and transient and several input variations. The resulting binary files are then converted to Matlab ® compatible files.
In a thermal FEM problem the energy equation is solved for each vol i using the first law of thermodynamics and can be written as [32]:

$$Cp_i m_i \cdot \frac{dT_i}{dt} = d_i\lambda_i \cdot (T_{i+1} + T_i) + \dot{Q}_i + A_i\alpha_i \cdot (T_{bc} - T_i) \tag{4}$$

Where Cp_i is the thermal capacity and m_i the mass of an element, λ_i is the heat conductivity with the element length d_i and α_i is the convective heat transfer of a boundary condition with an adjacent temperature T_{bc} and area A_i. $\dot{Q}_i$ is the heat source or heat generated inside the element. Combining Equation 3 and 4 results in the following state space representation of a thermal problem with the temperature as state variable.

$$\begin{aligned}\dot{\mathbf{T}}(t) =& \mathbf{E}^{-1}\mathbf{A}\mathbf{T}(t) + \mathbf{E}^{-1}\mathbf{B}\mathbf{q}(t)\\ \mathbf{y}(t) =& \mathbf{C}^T\mathbf{T}(t)\end{aligned} \tag{5}$$

Matrix E represents the thermal capacity Cp_i of each element and is assumed to be invertible, matrix A describes the conductive heat transferred to neighbor elements (λ_i) and constant boundary conditions as convective heat transfer (α_i). The matrix B describes the dependence on input variables such as variable boundary conditions (α_i) and heat sources ($\dot{Q}_i$) of the system [12].
Two possible MOR methods will be considered and compared in their accuracy and suitability for this application in the future, balanced truncation and padé approximation. In balanced truncation a system as described in 3 is considered. The aim is to find a projector T to build a balanced realization of the system and truncate the system based on the largest eigenvalues of the balanced gramians. Smaller singular values contribute to a small amount of energy transferred from the input u(t) to the output y(t) and thus can be truncated. The first r values are assumed to

contain most of the energy of the system. Especially for large linear and thermal systems balanced truncation has been established [33, 12, 34]. The resulting linear and time-invariant ROM can be described as following, where the dimension r of the reduced system matrices being significantly lower than n ($r \ll n$) [35, 29].

$$\begin{aligned} \dot{\mathbf{x}}(t) &= \mathbf{A}_r \mathbf{x}(t) + \mathbf{B}_r \mathbf{u}(t) \\ \mathbf{y}(t) &= \mathbf{C}_r^T \mathbf{x}(t) \end{aligned} \tag{6}$$

The thermal ROM calculates the temperature of the battery system of all electrical components T_{comp} based on the heat input $\dot{Q}_{\text{el}}$ from the electro-thermal model and the boundary conditions α_{fluid} and T_{fluid} at the cooling plate. Also, the heat flux $\dot{Q}_{\text{cooling}}$ to the cooling plate is calculated.

Approximation of the Cooling Plate and Fluid

The cooling plate is simulated in a CFD software (ANSYS Fluent ®). The model is meshed using a polyhedral mesh with 22 million cells. Here energy, momentum and mass equations are solved, resulting in a complex nonlinear system. Since the model is used only to calculate the heat transfer from the battery system into the fluid several assumptions and simplifications can be made to the sub model. It is for example not necessary for the overall goal to calculate the velocity, temperature and pressure of the cooling plate and cooling fluid precisely.

For the fluid a fully developed flow is assumed at every time step at a certain flow rate and temperature. Through this

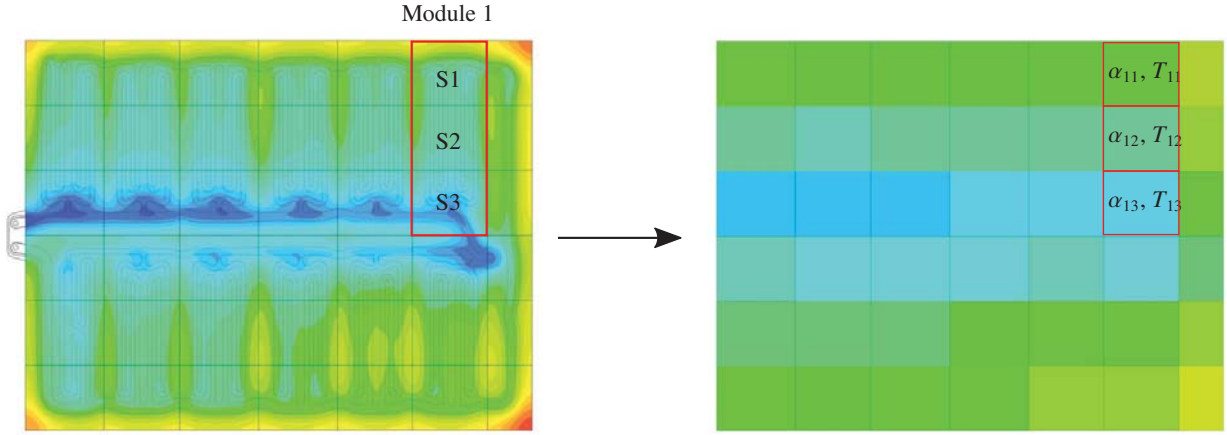

FIGURE 7. Approximation of the fluid cooling plate by calculating averaged values of heat transfer coefficient α and Temperature T at three surfaces (S1, S2 and S3) per module interface

assumption it is possible to calculate the flow stationary, with velocity and pressure values independent from time. In the fluid model heat transfer coefficients α_{fluid} and temperatures T_{fluid} are calculated at the interface of the cooling plate to the battery modules. The values are averaged over three areas per module interface to represent the different flow sections of the cooling plate. The simplification is shown in Figure 7.

For the validation the fluid model was simulated with a constant heat input from the battery system. The averaged values of temperature and heat transfer coefficient were obtained from the simulations. Those values were then applied to the thermal battery system model as boundary conditions and the temperatures inside the battery system were evaluated and compared to the complete model. Based on the previous assumptions an error of 0.77 °C is estimated in the batteries temperatures when comparing the full model and the decoupled model.

To create a fluid reduced order model Proper Orthogonal Decomposition (POD) is proposed. For this method snapshots are calculated from the fluid model at each input parameter set using a design of experiments (DOE) [36, 37]. Here input parameters are the fluid temperature at the inlet T_{fluid}, the mass flow rate at the inlet $\dot{m}_{\text{fluid}}$ and the heat flux from the 12 modules. Using those snapshots a set of POD modes and function parameters are calculated that can reproduce the input - output correlation. Another possibility is to use a neural network on the generated data. The output parameters from the fluid model will be then coupled to the thermal model. The three resulting sub models are connected through the described variables in Figure 6.

CONCLUSION

The modeling of battery systems remains an important engineering task for the development of electric vehicles in order to better understand and estimate the thermal and electrical behavior of battery cells.
As shown in this paper a coupled thermal and thermo-electric model can accurately depict the thermal behavior of the battery cells. The coupling of the ECM and the thermal model can predict the thermal behavior inside the battery cells with a mean deviation of 3.8 % from test data. A validation of the complete battery system model will be conducted with test data and using the software and modeling approaches as described in this paper.
A new modeling approach was discussed for the application of reduction techniques for multiphysical systems. By separating the original HDM into three sub models simple and established model order reduction methods can be applied onto each model. The coupling of the ECM and thermal model is done equivalent to the approach used in the HDM. Further, it was proven that the approximation of the cooling plate through averaged surface values is sufficiently accurate for the application and coupling with the thermal model.
The proposed methods are yet to be studied and compared for the application. Challenges in future work include the approximation of the thermal model though reduction techniques with multiple inputs and outputs and reducing the large model to real-time capable model size.

REFERENCES

[1] C. Julien, A. Mauger, A. Vijh, and K. Zaghib, in *Lithium Batteries: Science and Technology* (Springer International Publishing, Cham, 2016), pp. 29–68.
[2] Z. Rao and S. Wang, Renewable and Sustainable Energy Reviews **15**, 4554–4571 (2011).
[3] M. A. Hannan, M. S. H. Lipu, A. Hussain, and A. Mohamed, Renewable and Sustainable Energy Reviews **78**, 834–854 (2017).
[4] S. C. Chen, C. C. Wan, and Y. Y. Wang, Journal of Power Sources **140**, 111–124 (2005).
[5] K. Yeow, H. Teng, M. Thelliez, and E. Tan, "3d thermal analysis of li-ion battery cells with various geometries and cooling conditions using abaqus," in *Proceedings of the SIMULIA community conference*, edited by ABAQUS Inc. (Dassault Systemes, 2012).
[6] X. Lin, H. Fu, H. E. Perez, J. B. Siege, A. G. Stefanopoulou, Y. Ding, and M. P. Castanier, Oil & Gas Science and Technology–Revue d'IFP Energies nouvelles **68**, 165–178 (2013).
[7] W. Li, M. Rentemeister, J. Badeda, D. Jöst, D. Schulte, and D. U. Sauer, Journal of Energy Storage **30**, p. 101557 (2020).
[8] B. Wu, W. D. Widanage, S. Yang, and X. Liu, Energy and AI p. 100016 (2020).
[9] E. O'Dwyer, I. Pan, R. Charlesworth, S. Butler, and N. Shah, Sustainable Cities and Society p. 102412 (2020).
[10] D. Ribbe-Sorano and R. Wendland, GermanVerfahren zum ueberpruefen eines in einem batteriesystem erfassten temperaturmesswertes und batteriesystem, January 2020 German Patent DE102018210411A1.
[11] D. Botto, S. Zucca, and M. M. Gola, Journal of Thermal Stresses **30**, 819–839 (2007).
[12] M. Salleras, T. Bechtold, L. Fonseca, J. Santander, E. B. Rudnyi, J. G. Korvink, and S. Marco, "Comparison of model order reduction methodologies for thermal problems," in *EuroSimE 2005. 6th International Conference on Thermal, Mechanial and Multi-Physics Simulation and Experiments in Micro-Electronics and Micro-Systems, 2005* (April 18-20, 2005), pp. 60–65.
[13] A. P. Raghupathy, "Boundary-condition-independent reduced-order modeling for thermal analysis of complex electronics packages," Ph.D. thesis, University of Cincinnati 2009.
[14] C. Rowley, International Journal of Bifurcation and Chaos **15**, 997–1013 (2005).
[15] G. Stabile, F. Ballarin, G. Zuccarino, and G. Rozza, Advances in Computational Mathematics 1–20May (2019).
[16] D. Xiao, F. Fang, C. Pain, and G. Hu, International Journal for Numerical Methods in Fluids **79**, 580–595 (2015).
[17] E. Rudnyi, *Grazer Symposium Virtuelles Fahrzeug*, Grazer Symposium Virtuelles Fahrzeug (2009).
[18] M. Muratori, M. Canova, Y. Guezennec, and G. Rizzoni, IFAC Proceedings Volumes **43**, 192–197 (2010).

[19] G. Fan, K. Pan, and M. Canova, "A comparison of model order reduction techniques for electrochemical characterization of lithium-ion batteries," in *54th IEEE Conference on Decision and Control*, edited by Y. Ohta and M. Sampei (2015), pp. 3922–3931.
[20] A. Sancarlos, M. Cameron, A. Abel, E. Cueto, J.-L. Duval, and F. Chinesta, Archives of Computational Methods in Engineering 1–37 (2020).
[21] S. S. Madani, M. J. Swierczynski, and S. K. Kær, "The discharge behavior of lithium-ion batteries using the dual-potential multi-scale multi-dimensional (msmd) battery model," in *2017 Twelfth International Conference on Ecological Vehicles and Renewable Energies (EVER)* (IEEE, 2017), pp. 1–14.
[22] G. Li, S. Li, and J. Cao, "Application of the msmd framework in the simulation of battery packs," in *ASME International Mechanical Engineering Congress and Exposition*, Vol. 46569 (American Society of Mechanical Engineers, 2014) p. V08BT10A026.
[23] F. Saidani, F. X. Hutter, R.-G. Scurtu, W. Braunwarth, and J. N. Burghartz, Advances in Radio Science **15**, 83–91 (2017).
[24] P. Vyroubal and T. Kazda, Journal of Energy Storage **15**, 23–31 (2018).
[25] S. Lin, S. Stanton, W. Lian, and T. X. Wu, "Battery modeling based on the coupling of electrical circuit and computational fluid dynamics," in *IEEE Energy Conversion Congress and Exposition (ECCE)* (2011), pp. 2622–2627.
[26] A. Grimm and A. Haumer, "Parametrization of a simplified physical battery model," in *Proceedings of the 13th International Modelica Conference*, edited by A. Haumer (2019), pp. 215–220.
[27] A. Szardenings, GermanVerfahren und vorrichtung zum ueberwachen eines elektrischen energiespeichers, computerprogramm produkt, German Patent DE 10 2020 203 004 A1, to be published in 2022.
[28] E. B. Rudnyi and J. G. Korvink, *Applied Parallel Computing. State of the Art in Scientific Computing*, Applied Parallel Computing. State of the Art in Scientific Computing 349–356 (2004).
[29] A. C. Antoulas and D. C. Sorensen, International Journal of Applied Mathematics and Comput.er Science **11**, 1093–1121 (2001).
[30] Z. Bai, Applied Numerical Mathematics **43**, 9–44 (2002).
[31] A. C. Antoulas, Annual reviews in Control **29**, 181–190 (2005).
[32] B. Weigand, J. Koehler, and J. von Wolfersdorf, *Thermodynamik kompakt*, 3rd ed. (Springer Berlin Heidelberg, 2013).
[33] J. Ma, S. J. Qin, and T. Salsbury, "Model predictive control of building energy systems with balanced model reduction," in *2012 American Control Conference (ACC)* (IEEE, 2012), pp. 3681–3686.
[34] T. Bechtold, "Model order reduction of electro-thermal mems," Dissertation, Albert-Ludwigs Universität, Freiburg im Breisgau 2005.
[35] P. Benner and A. Schneider, *Balanced truncation for descriptor systems with many terminals* (Max Planck Institute for Dynamics of Complex Technical Systems, 2013).
[36] C. W. Rowley, T. Colonius, and R. M. Murray, Physica D: Nonlinear Phenomena **189**, 115–129 (2004).
[37] K. Willcox and J. Peraie, American Institute of Aeronautics and Astronautics Journal **40**, 2323–2330 (2002).